Published OnlineFirst June 23, 2009; DOI: 10.1158/0008-5472.CAN-08-4625

Research Article

# The Liver Is a Site for Tumor-Induced Myeloid-Derived Suppressor Cell Accumulation and Immunosuppression

Dan Ilkovitch[1] and Diana M. Lopez[1,2]

[1]Department of Microbiology and Immunology and [2]Sylvester Comprehensive Cancer Center, Miller School of Medicine, University of Miami, Miami, Florida

## Abstract

**Tumor-induced immunosuppression plays a key role in tumor evasion of the immune system. A key cell population recognized as myeloid-derived suppressor cells (MDSC) contributes and helps orchestrate this immunosuppression. MDSC can interact with T cells, macrophages, and natural killer cells to create an environment favorable for tumor progression. In various tumor models, their presence at high levels has been reported in the bone marrow, blood, spleen, and tumor. We report for the first time that MDSC accumulate and home to the liver in addition to the other organs. Liver MDSC suppress T cells and accumulate to levels comparable with splenic MDSC. Additionally, hematopoiesis in the liver contributes to the dramatic expansion of MDSC in this organ. Furthermore, MDSC in the liver interact with macrophages, also known as Kupffer cells, and cause their up-regulation of PD-L1, a negative T-cell costimulatory molecule. The liver is thus an organ in which MDSC accumulate and can contribute to immunosuppression directly and indirectly. MDSC play a role in various pathologic states in addition to cancer, and these results contribute to our understanding of their biology and interactions with immune-related cells.** [Cancer Res 2009;69(13):5514–21]

## Introduction

Tumor-induced immunosuppression is accepted as a key mechanism by which tumors evade the immune system. This is a critical capability which tumors gain in the last stage of the immunoediting process (1). Nearly 20 years ago, we described hematopoietic changes in tumor-bearing mice involving myeloid cells which accumulate in the spleen due to tumor-derived factors (2). We reported that these $CD11b^+$ (MAC-1) cells down-regulate polyclonal and antigen-specific T-cell and B-cell responses (3). These cells, now described as $CD11b^+GR\text{-}1^+$ myeloid-derived suppressor cells (MDSC), suppress T cells in various cancer models (4, 5) and patients (6). These cells have also been described in other pathologic states, including inflammatory bowel disease (7), traumatic stress (8), burns (9), infection (10), and transplantation (11).

Besides suppressing $CD4^+$ and $CD8^+$ T cells, MDSC interact with other immune regulatory cells (12), and block antitumor immunity. They have been found to block natural killer cell cytotoxicity (13), they modulate macrophages to an immunosuppressive M2 phenotype (14), and can induce the development of T regulatory cells ($T_{reg}$; ref. 15). We discovered that MDSC home to and accumulate in high numbers in the liver. Furthermore, the dramatic increase in systemic levels of MDSC in tumor-bearers is in part explained by extramedullary hematopoiesis, as increased levels of hematopoietic progenitors exist in the spleen and liver. We also report for the first time that in tumor-bearers, the liver plays a critical role in immunosuppression by accumulating MDSC which interact with liver macrophages, or Kupffer cells, and inducing high levels of the negative T-cell costimulatory molecule PD-L1 on their surface.

## Materials and Methods

**Animals/cell lines.** BALB/c mice ($H\text{-}2^d$) were bred in our animal facility at the University of Miami according to NIH guidelines. C57BL/6 mice were purchased from the Jackson Laboratory. DO11.10 transgenic mice were kindly provided by Dr. Becky Adkins (University of Miami, Miami, FL). The DA-3 mammary tumor cells were maintained as previously described (2). The 4T1 cell line was kindly provided by Dr. Fred Miller (Wayne State University, Detroit, MI). B16.F10 and Lewis lung carcinoma (LLC) cells were purchased from American Type Culture Collection. Tumor cells ($1 \times 10^6$ DA-3, $1 \times 10^4$ 4T1, and $2.5 \times 10^5$ B16 or LLC) were injected s.c., and then 4-wk-old to 5-wk-old tumor-bearing animals were used for the indicated studies. Recombinant murine granulocyte macrophage–colony-stimulating factor (GM-CSF; R&D Systems) was injected i.p. in 0.9% saline. For the *in vivo* PD-L1 experiment, mice inoculated with DA-3 cells s.c. were administered i.p. with either saline or 150 μg of anti–PD-L1 (BioLegend) every 3 to 4 d, while tracking tumor development.

**Cell harvesting/purification.** Spleens were mashed through 70 μmol/L cell strainers (BD Biosciences) to obtain single-cell suspensions. Liver leukocytes were harvested by removing livers, chopping them to pieces, and resuspending in 4.5 mL of HBSS and 350 μL of digestion enzyme mixture provided in a protocol by Dr. Alan B. Frey (New York University, New York, NY; ref. 16). The stock digestion enzyme mixture consisted of 5 mg/mL of collagenase I, 5 mg/mL of collagenase IV, 2.5 mg/mL of hyaluronidase V (Sigma-Aldrich), and 1 mg/mL of DNase I (Roche). Tissue/enzyme mixture was placed in a 37°C shaker for 30 min, then poured through 70 μmol/L cell strainers (BD Biosciences). To remove hepatocytes, cells were resuspended in 1.2 mL of RPMI, and 2.8 mL of 50% Histodenz (Sigma-Aldrich) solution in PBS, and underlaid in tubes containing 2.0 mL of RPMI. Mixture was centrifuged for 20 min at $1,500 \times g$, at 5°C. Interphase cells were removed and washed using RPMI. Purification of MDSC/Kupffer cells was performed by staining cells using anti–GR-1 (RB6-8C5; BD Biosciences) or anti-F4/80 (Invitrogen), respectively, followed by magnetic antibody cell separation using goat anti-rat microbeads (Miltenyi Biotec). For negative selection of MDSC, cells were stained with biotin-conjugated anti-CD4, anti-CD8, and anti-CD45 from BD Biosciences, followed by separation using BD IMag SAv particles (BD Biosciences).

**Imaging.** Cells were labeled with 2 μmol/L of DiR (Invitrogen; ref. 17). In other experiments, 40 μg of anti–GR-1.APC-Cy7 (BD Biosciences) were injected i.v. Mice were imaged and analyzed using an optical bioimager (IVIS 200; Xenogen) with Ex/Em of 745/820 nm for DiR or 640/800 nm for APC-Cy7.

**Pathology.** Paraffin embedding, sectioning, and staining with H&E was performed at the Comparative Pathology Laboratory (University of Miami).

**Requests for reprints:** Diana M. Lopez, Department of Microbiology and Immunology, Miller School of Medicine, University of Miami, P.O. Box 016960 (R-138), Miami, FL 33101. Phone: 305-243-6632; Fax: 305-243-4409; E-mail: dlopez@med.miami.edu.



doi:10.1158/0008-5472.CAN-08-4625

Published OnlineFirst June 23, 2009; DOI: 10.1158/0008-5472.CAN-08-4625



To analyze purified MDSC, $1 \times 10^6$ cells were dried onto slides, fixed in methanol, and stained using Harleco Hemcolor (EMD Chemicals). Immunohistochemistry was performed by fixing cryopreserved liver sections in cold acetone for 5 min, allowing to air-dry, and after rehydrating with PBS and blocking with antibody diluent (BD Biosciences), sections were stained with anti–GR-1.APC and anti-CD11b.FITC. Sections were then washed thoroughly and coverslipped with VectaShield 4′,6-diamidino-2-phenylindole mounting medium (Vector Laboratories). Slides were analyzed and photographed using a Zeiss LSM510/UV inverted confocal microscope at the Analytical Imaging Core Facility (University of Miami).

**Flow cytometry.** Cells were Fc blocked and antibody-labeled in fluorescence-activated cell sorting buffer (PBS, 0.5%bovine serum albumin, 0.1% sodium azide), then analyzed on an LSR II (BD Biosciences). Antibodies used included anti–GR-1.APC, anti-CD11b.PE, anti–PD-L1.PE, anti–CD4.PE-Cy5 from BD Biosciences, anti-F4/80.FITC from Invitrogen, and anti–B7-H4.PE from eBioscience.

**Hematopoiesis/clonogenic assay.** Cell suspensions were diluted to $2 \times 10^5$ cells/mL in Iscove's modified Dulbecco's medium with 2% heat-inactivated FCS for mouse myeloid colony-forming cells (StemCell Technologies) and 10× penicillin/streptomycin. Cell solution (0.3 mL) was then mixed with MethoCult GF M3434 (3 mL) for CFU-GEMM clonogenic potential, or MethoCult M3001 for CFU-GM clonogenic potential (StemCell Technologies). Cells were then plated in duplicate at 1 mL per well in six-well dishes and incubated for 11 d before scoring the number of colonies.

**Suppression assay/Kupffer cell assay.** DO11.10 splenocytes were labeled with 2.5 μmol/L of 5-(and 6) carboxyfluorescein diacetate succinimidyl ester (CFSE) for 10 min at 37°C. Labeled splenocytes were plated at $2 \times 10^5$ cells per well in flat-bottomed 96-well plate, in HL-1 medium (Bio Whittaker) containing penicillin/streptomycin, glutamax, and 2-ME. Ovalbumin (EMD/Calbiochem) was added at 15 μg/mL. MDSC purified by magnetic antibody cell separation were added at the indicated concentrations. After 5 d, cells labeled with anti-CD4 were analyzed for CFSE dilution. For Kupffer assays, DO11.10 splenocytes were preactivated with 50 μg/mL of ovalbumin for 8 d. T-cells were purified using magnetic antibody cell separation CD90 beads and cocultured ($2 \times 10^5$) with Kupffer cells ($5 \times 10^4$), or splenic dendritic cells purified using magnetic antibody cell separation CD11c beads in the presence of 5 μg/mL of ovalbumin. $F(ab')_2$ fragments of anti–PD-L1 (BioLegend) or isotype were made using $F(ab')_2$ micro-preparation kit (Pierce), and added to cultures at 10 μg/mL. IFN-γ was analyzed in 4-d-old cultures by ELISA (BD Biosciences).

## Results

**MDSC home to and accumulate in the liver.** MDSC ($CD11b^+GR\text{-}1^+$) have been reported at high levels in spleen, bone marrow, and blood of tumor-bearing mice, as well as in infiltrating primary tumors. To investigate MDSC homing, splenic MDSC were isolated from BALB/c mice harboring mammary DA-3 tumors, and labeled with a near-IR dye (DiR). MDSC were then injected ($4 \times 10^6$) i.v. into either normal or tumor-bearing mice. After 24 hours, the mice were imaged using a bioimager, and displayed the highest intensity in the spleen and livers of both tumor-bearing and normal mice (Fig. 1*A*). MDSC have not been previously described to home to the liver; however, it is also possible that dead cells or released dye accumulate for removal by the liver (17). To determine whether MDSC actually accumulate in the liver of tumor-bearing mice, normal BALB/c mice or mice harboring a DA-3 tumor were injected i.v. with an antibody against GR-1 (anti–GR-1.APC-Cy7), and imaged using a bioimager 20 minutes later. A high intensity of labeling was found in tumor-bearers relative to normal mice, with 1.8-fold, 7.3-fold, and 11.5-fold higher signals from the liver, spleen, and bones, respectively (Fig. 1*B*). Some signals from the liver are due to the removal of antibodies; however, signals from the livers of tumor-bearing mice were higher than that of normal livers.

To analyze further whether MDSC accumulate in the livers of tumor-bearing mice, livers from normal mice or DA-3 tumor–bearers were isolated, fixed in formalin, and embedded in paraffin. In livers from tumor-bearers, large nests of leukocytes could be detected perivascularly as well as throughout the liver parenchyma (Fig. 1*C*). Frozen sectioning of liver tissue reveals the nuclei of these cells, which are characteristic of MDSC that are a heterogeneous population of cells including immature myeloid cells with rounded nuclei, bands, and macrophages (Fig. 2*A*). Liver histology was also performed on livers from other tumor models, and the same nest pattern was observed in the livers of 4T1 tumor–bearing mice (Fig. 2*B*). Although the DA-3 model is not metastatic to the liver, the 4T1 model does metastasize to the liver, and interestingly, some metastatic nodules were surrounded by MDSC (Fig. 2*B*). To further characterize these nests of leukocytes, immunohistochemistry was performed by staining cryopreserved sections using antibodies to GR-1 and CD11b. Sections of liver from tumor-bearers showed clusters of intense staining for these two markers, whereas sections of normal livers showed no colocalized staining (Fig. 2*C*). MDSC were then purified from the liver and spleens of 4T1 tumor–bearers and stained on slides for comparison, and were similar histologically (Fig. 2*D*).

**The liver accumulates high levels of suppressive MDSC, comparable with the spleen.** Systemic levels of MDSC have been correlated to tumor burden, likely due to the levels of tumor-derived factors shown to stimulate their production and prevent their maturation (2). To investigate how levels of MDSC in the liver compare to the spleen, paired livers and spleens from tumor-bearing and normal animals were harvested, and cells double-stained for CD11b and GR-1, and analyzed by flow cytometry. Two BALB/c tumor models, DA-3 and 4T1, and two C57BL/6 tumor models, B16 melanoma and LLC, were analyzed. In all four tumor models, levels of MDSC in the liver paralleled those in the spleen in a linear fashion (Fig. 3*A*). Normal livers resembled normal spleens, with low levels of MDSC at 2% to 5%, whereas tumor-bearers' livers resembled tumor-bearers' spleens (Fig. 3*B*). A T-cell suppression assay was performed using MDSC purified from either the liver or spleen of the same tumor-bearing animal. CFSE labeled splenocytes from DO11.10 transgenic mice were stimulated with ovalbumin in the absence or presence of MDSC from the two organs. Liver MDSC suppression of T-cell proliferation was comparable to splenic MDSC suppression, with 80% suppression at a 1:1 ratio of splenocytes to MDSC, as seen by the lack of CFSE dilution in DO11.10 $CD4^+$ T-cells (Fig. 3*C*).

**MDSC accumulation is in part due to increased hematopoiesis in the liver.** In Fig. 1, we showed that MDSC adoptively transferred into either normal or tumor-bearing mice accumulated in the spleen and liver of both animals. Furthermore, using tumor models which do (4T1) or do not (DA-3) metastasize to the liver, we found that MDSC accumulate in the liver irrespective of liver metastatic disease. However, MDSC accumulation in the spleen and liver could be a result of tumor-derived factors. We reported in the past that tumor production of GM-CSF could lead to the hematopoietic changes and immune dysfunction observed in tumor-bearing mice, including the splenic accumulation of MDSC (2, 18). We thus investigated whether the accumulation of MDSC by GM-CSF could lead to liver MDSC accumulation. BALB/c mice were injected i.p. with 5 μg of GM-CSF twice daily for 3 days, and then spleens and livers were harvested and analyzed for levels of MDSC. Although saline-injected control mice harbored low levels of MDSC in both the spleen and the liver, GM-CSF–injected mice had up-regulated levels of MDSC in both the spleen and liver (Fig. 4*A*).

Other investigators have previously reported that expansion of myeloid cells in tumor-bearing mice was in part due to either

Published OnlineFirst June 23, 2009; DOI: 10.1158/0008-5472.CAN-08-4625



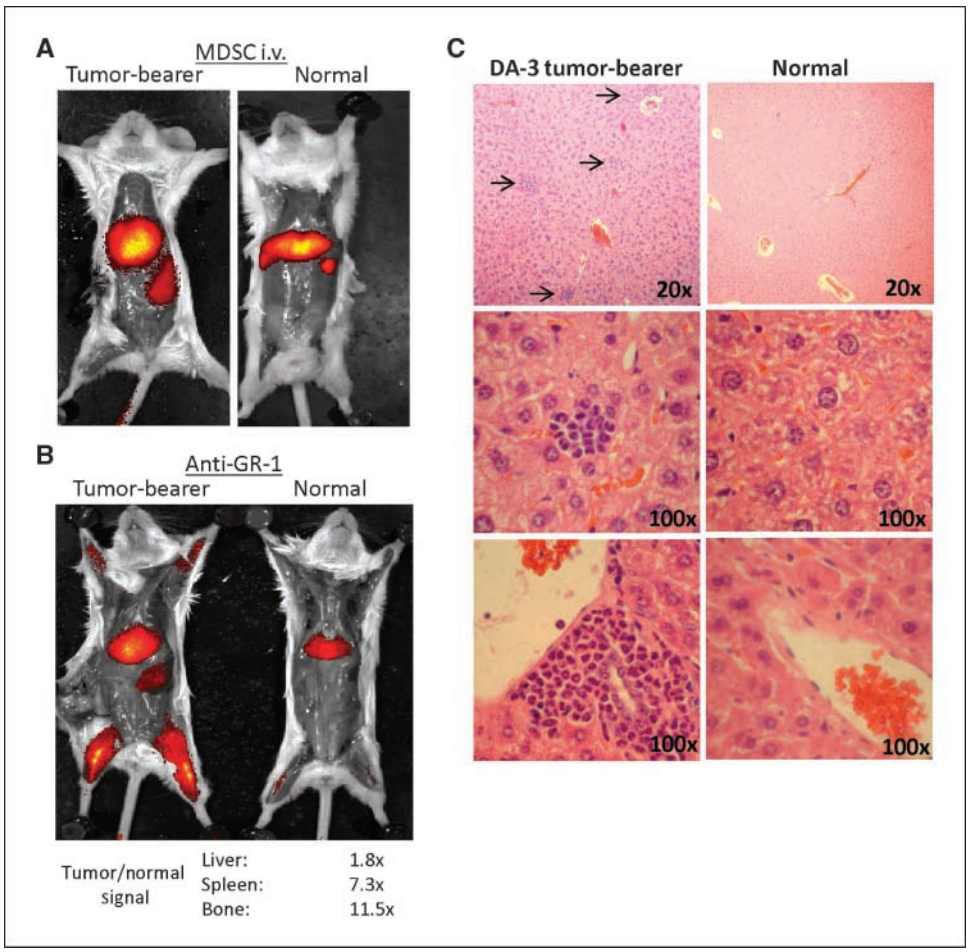


**Figure 1.** MDSC home to the liver. *A,* splenic MDSC were purified from DA-3 tumor–bearers and labeled with DiR dye. MDSC were injected ($4 \times 10^6$) i.v. into normal mice or DA-3 tumor–bearers, and imaged 24 h later. *B,* DA-3 tumor–bearing or normal mice were injected i.v. with anti–GR-1.APC-Cy7 and imaged 20 min later. Fold increase in signal intensity in tumor-bearers relative to normal mice is indicated. *C,* paraffin sections of livers from normal or DA-3 tumor–bearers were stained with H&E. *Arrows*, nests of MDSC; magnification is indicated in the figures. Data are representative of at least three experiments.

increased hematopoietic progenitors colonizing the spleen, or increased splenic hematopoiesis (19). Furthermore, because nests of leukocytes were detected throughout the liver, we tested the clonogenic activity in livers, spleens, and bone marrow of DA-3 tumor–bearers and in normal mice. The number of hematopoietic colonies, whether assaying early progenitors (CFU-GEMM) or more differentiated progenitors (CFU-GM), were greatly increased from all three compartments of tumor-bearing mice relative to those from normal mice (Fig. 4*B*). Thus, MDSC likely arise from all three sites, contributing to their dramatic accumulation systemically, and specifically in these organs.

**MDSC up-regulate PD-L1 on liver Kupffer cells.** Liver macrophages, known as Kupffer cells, are involved in the induction of immunologic tolerance (20), and in the resolution of infections and liver pathology. Mechanisms used in the induction of tolerance by these cells include cytokine secretion and expression of inhibitory costimulatory molecules, such as PD-L1 (CD274, B7-H1). We investigated the phenotype of F4/80$^+$ Kupffer cells and splenic macrophages in DA-3 tumor–bearing and normal mice for surface expression of two T-cell inhibitory costimulatory molecules, PD-L1 and B7-H4 (21). Although PD-L1 is constitutively expressed on liver and spleen F4/80$^+$ cells of normal animals, it is 2-fold higher on Kupffer cells from tumor-bearing mice (Fig. 5*A*). PD-L1 was also higher in Kupffer cells of B16 tumor–bearing mice (data not shown). Furthermore, this is a Kupffer cell–specific phenotype, as splenic macrophages expressed the same levels of PD-L1 from either tumor-bearing or normal mice. B7-H4 was expressed at lower levels, but was identical on macrophages from tumor-bearers and normal mice (Fig. 5*A*). Because MDSC accumulate in the livers of tumor-bearers, we investigated whether MDSC induce higher Kupffer cell PD-L1 expression. Adoptive transfer of purified splenic MDSC from tumor-bearers i.v. into normal BALB/c mice leads to a rapid increase in Kupffer cell surface PD-L1 (at 2 and 5 hours; Fig. 5*B*), and returns to baseline within 20 hours, likely due to the absence of a tumor-bearing immunosuppressive environment. To investigate whether the up-regulation of PD-L1 on Kupffer cells by MDSC was specifically due to MDSC derived from tumor-bearers, or whether MDSC from normal animals, if given at the same high numbers, could also up-regulate this immunosuppressive molecule, pooled normal or tumor splenic MDSC were adoptively transferred into normal mice. After 5 hours, the livers were analyzed for levels of MDSC and PD-L1 expression on Kupffer cells. Although saline-injected mice harbored ~3% MDSC within the liver, mice adoptively transferred with either tumor or normal MDSC harbored 14% to 15% MDSC within the liver (data not shown). PD-L1 was up-regulated on Kupffer cells in the presence of MDSC, irrespective of their origin from either tumor or normal mice (Fig. 5*C*). It is also important to note that in our tumor models, MDSC are negative for both PD-L1 and F4/80 (data not shown).

**PD-L1 up-regulation contributes to immunosuppression.** PD-L1 has been shown to interact with its receptor PD-1, which is up-regulated on activated T-cells, and suppress T-cell IFN-γ production (22). To confirm this negative costimulatory function, we cultured preactivated DO11.10 T-cells in the presence of

Published OnlineFirst June 23, 2009; DOI: 10.1158/0008-5472.CAN-08-4625



ovalbumin, with normal or tumor-bearers' Kupffer cells, or normal splenic dendritic cells as a control. In the presence of PD-L1 blocking $F(ab')_2$ fragments, the secretion of IFN-γ by T-cells cocultured with Kupffer cells can be up-regulated (Fig. 6*A*). Dendritic cells, on the other hand, efficiently activate T-cells and thus induce a higher production of IFN-γ. There is a lower production of IFN-γ in the presence of tumor Kuppfer cells relative to the presence of normal Kupffer cells (~600 pg/mL difference). Although we would have predicted a bigger difference based on PD-L1 expression, as it turns out, Kupffer cell adherence to plastic *in vitro* causes PD-L1 to completely down-regulate within an hour and then to up-regulate to similar levels after several hours *in vitro* (data not shown). Although we cannot selectively down-modulate PD-L1 on Kupffer cells, we investigated whether *in vivo* blockade of this ligand systemically in tumor-bearers had any effect on tumor growth. DA-3 tumor–bearing mice receiving anti–PD-L1 treatments twice weekly showed slowed tumor growth relative to mice receiving saline (Fig. 6*B*). As shown by others, breaking the PD-1/PD-L1 axis alone can slow the growth and metastasis of some tumor models (23, 24). However, it has been shown to be markedly more effective in combination with other antitumor immunotherapies (24, 25).

## Discussion

MDSC are now recognized as key players of immunosuppression in cancer and other chronic inflammatory pathologies. Specifically in cancer, they have been found to expand in almost every mouse model (26), and in various human cancers, including melanoma (27), breast (28), lung (29), renal cell carcinoma (30), and

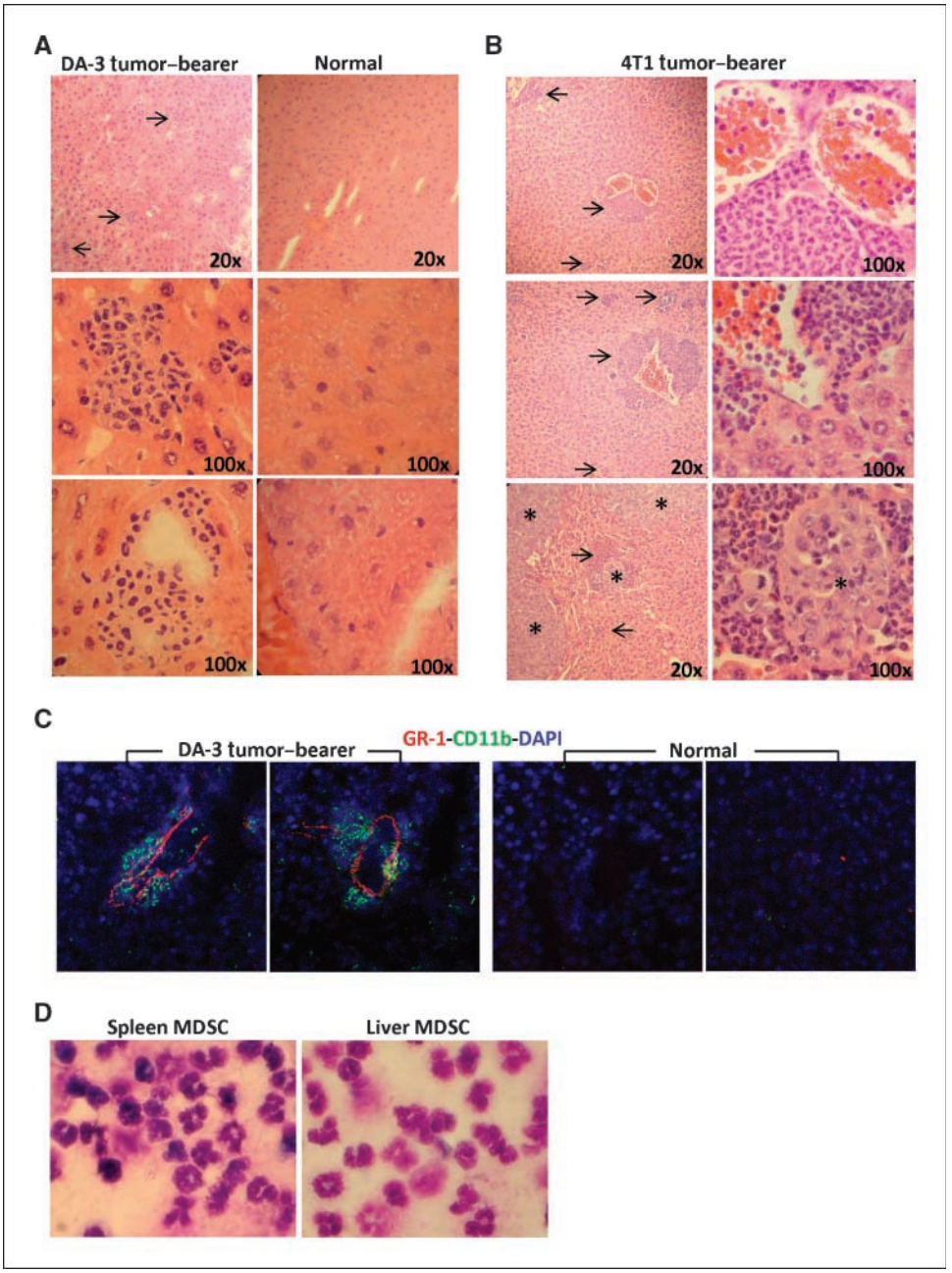


**Figure 2.** MDSC form nests in livers of tumor-bearers. *A,* frozen sections of livers from normal or DA-3 tumor–bearers; *B,* paraffin sections of liver from 4T1 tumor–bearers were stained with H&E. *C,* immunohistochemistry for CD11b (*green*), GR-1 (*red*), and 4′,6-diamidino-2-phenylindole (DAPI) staining was performed on frozen sections of livers from normal and DA-3 tumor–bearers. *D,* purified liver and splenic MDSC from 4T1 tumor-bearers were stained for histology. *Arrows*, nests of MDSC; *, metastatic nodules in the liver; magnification is indicated in the figures. Data are representative of four specimens or experiments.

Published OnlineFirst June 23, 2009; DOI: 10.1158/0008-5472.CAN-08-4625



hepatocellular carcinoma (31). We and others previously reported that they accumulate due to tumor-derived factors (2), and suppress T cells in a cell contact–dependent manner (3). Although the mechanisms of their suppressive activity, such as arginase expression (32), and their expansion and recruitment by tumor-derived factors, such as GM-CSF (2, 18, 33), urokinase plasminogen activator (34), and stem cell factor (35) are being uncovered, much of their biology remains to be elucidated. Because MDSC accumulation has been reported in the spleen, bone marrow, blood, and within the tumor, we set out to determine where MDSC preferentially home. MDSC adoptively transferred into either normal or tumor-bearing mice homed mainly to the liver and

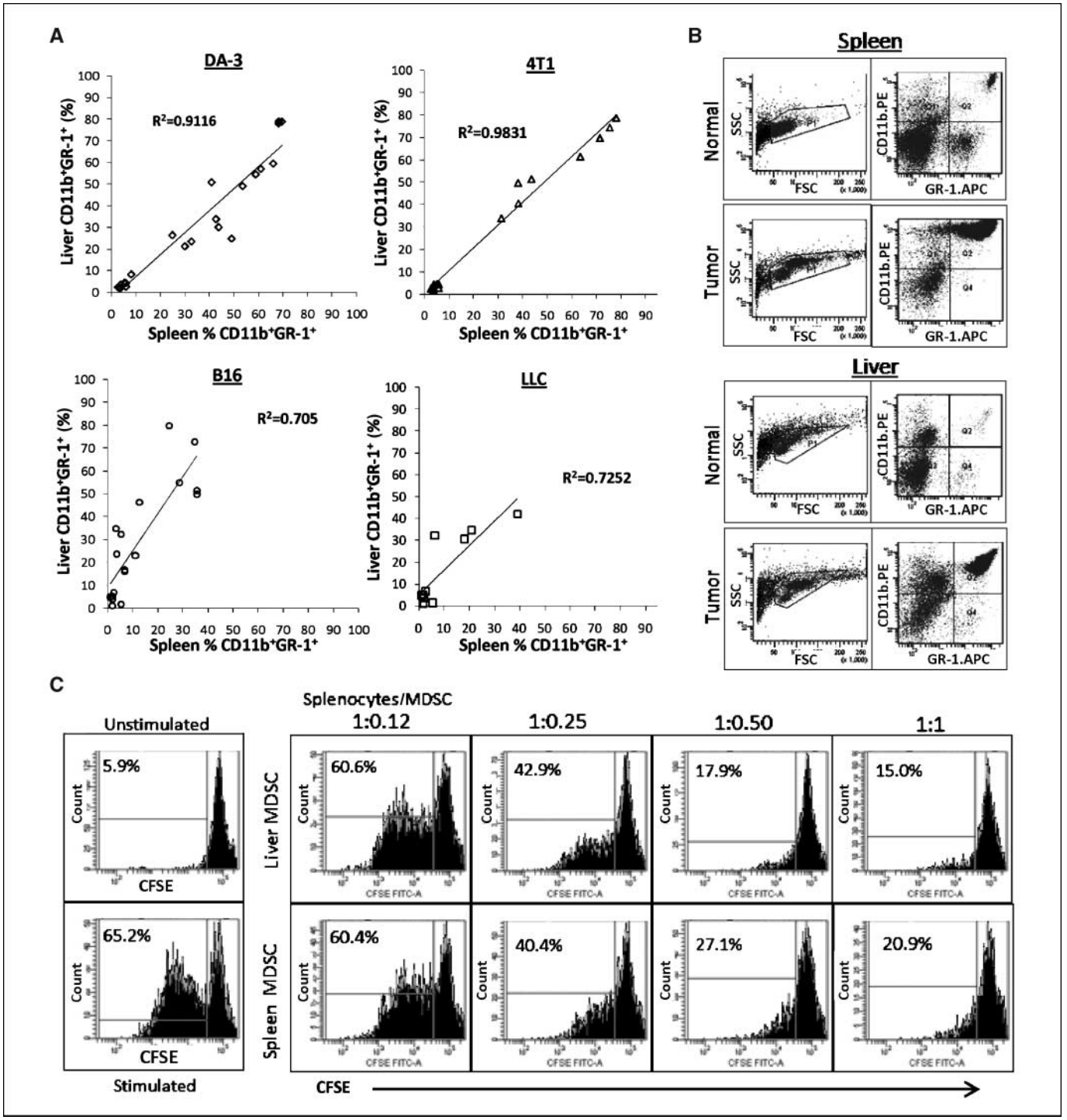


**Figure 3.** Liver MDSC accumulation is comparable to the spleen. *A,* liver and spleen cells from BALB/c mice harboring DA-3 or 4T1 tumors, or C57BL/6 mice harboring B16 or LLC tumors were stained for CD11b and GR-1 and analyzed by flow cytometry. Each symbol indicates paired liver and spleen from one mouse. *B,* flow cytometry profiles of MDSC accumulation in spleen and liver of normal mice and DA-3 tumor–bearers. *C,* CFSE-labeled DO11.10 splenocytes were stimulated with ovalbumin in the absence or presence of MDSC, and purified from liver or spleen of DA-3 tumor–bearers at the indicated ratios. CFSE dilution is presented by gating on $CD4^+$ cells. Data is representative of three experiments.

Published OnlineFirst June 23, 2009; DOI: 10.1158/0008-5472.CAN-08-4625



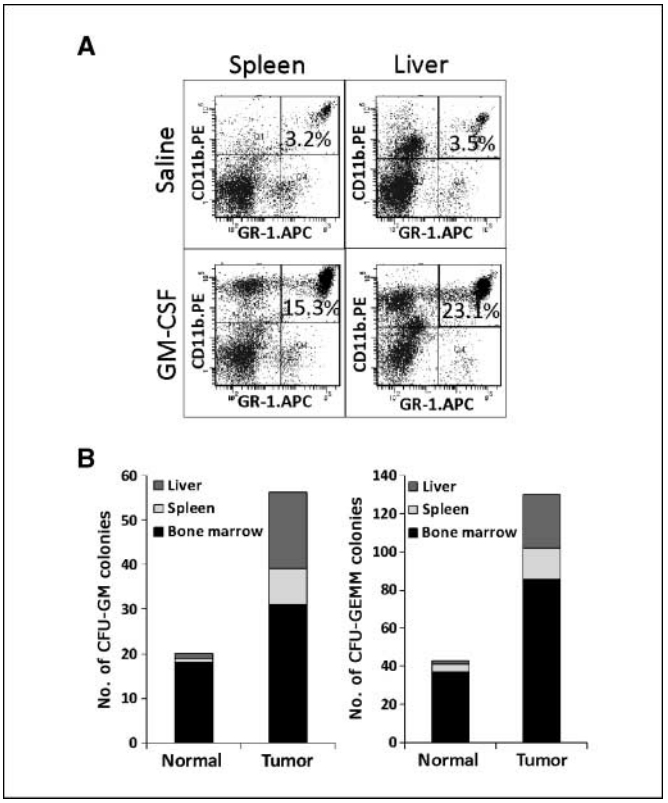


**Figure 4.** MDSC expansion is in part due to hematopoiesis in the spleen and liver. *A,* liver and spleen cells from BALB/c mice injected twice daily for 3 d with 5 μg of GM-CSF i.p., or saline as control, were stained for CD11b and GR-1 and analyzed by flow cytometry. *B,* liver, spleen, and bone marrow cells were harvested from normal or DA-3 tumor–bearing mice and tested for clonogenic activity of either early progenitors (CFU-GEMM) or more differentiated progenitors (CFU-GM) which lead to myeloid cell production. Data is representative of three experiments.

spleen (Fig. 1*A*). Because MDSC had not been previously described to home to the liver, we investigated whether MDSC normally accumulate in the livers of tumor-bearing mice. Injecting a fluorescently labeled GR-1 antibody detected by a bioimager, we found that greater levels of antibody were detected in the livers of tumor-bearers, relative to those of normals, as well as in the bone and spleen as previously described sites of MDSC accumulation (Fig. 1*B*). The histology of the livers from tumor-bearers show nests of myeloid cells perivascularly as well as throughout the liver parenchyma of tumor-bearers (Figs. 1*C* and 2), and flow cytometry confirmed the presence of high levels of $CD11b^+GR\text{-}1^+$ cells (Fig. 3).

There have been previous reports of hematopoiesis in the livers of tumor-bearers, but the cells were either not specifically identified or labeled as granulocytes, and more importantly, were attributed to liver metastatic disease by the 4T1 breast tumor model (36, 37). More recently, Li and colleagues have identified MDSC accumulation in the liver of an orthotopic liver cancer model, in which tumor cells are injected directly into the liver (38). Although there have been several reports like these of MDSC within tumors, and being recruited to tumor cells, our data show that MDSC accumulate in the livers of both tumor models with metastatic disease to the liver (4T1), and in the absence of liver metastatic disease (DA-3, B16, and LLC). We also showed that liver MDSC are functionally suppressive of T-cell proliferation, similar to those from the spleen (Fig. 3*C*). Furthermore, GM-CSF, which has been shown to be secreted by various human and mouse cancers, was able to expand MDSC in livers in the absence of a growing tumor (Fig. 4A). Although we showed in Fig. 1 that MDSC home to the liver after adoptive transfer, based on the nesting pattern on liver histology, it raised the possibility that MDSC could also be arising from the liver. Other groups have shown that splenic hematopoiesis, by the presence of myeloid progenitors and their clonogenic activity, was highly up-regulated in tumor-bearers (19). We confirmed that the bone marrow and spleen had high levels of hematopoietic activity, but also found that the liver likewise has higher activity in tumor-bearing mice (Fig. 4B). Thus, all these sites contribute to the expansion of MDSC in these organs.

We and others have shown that macrophages in tumor-bearers are altered systemically (39–41), and because the liver is a site for macrophages known as Kupffer cells, we analyzed whether their

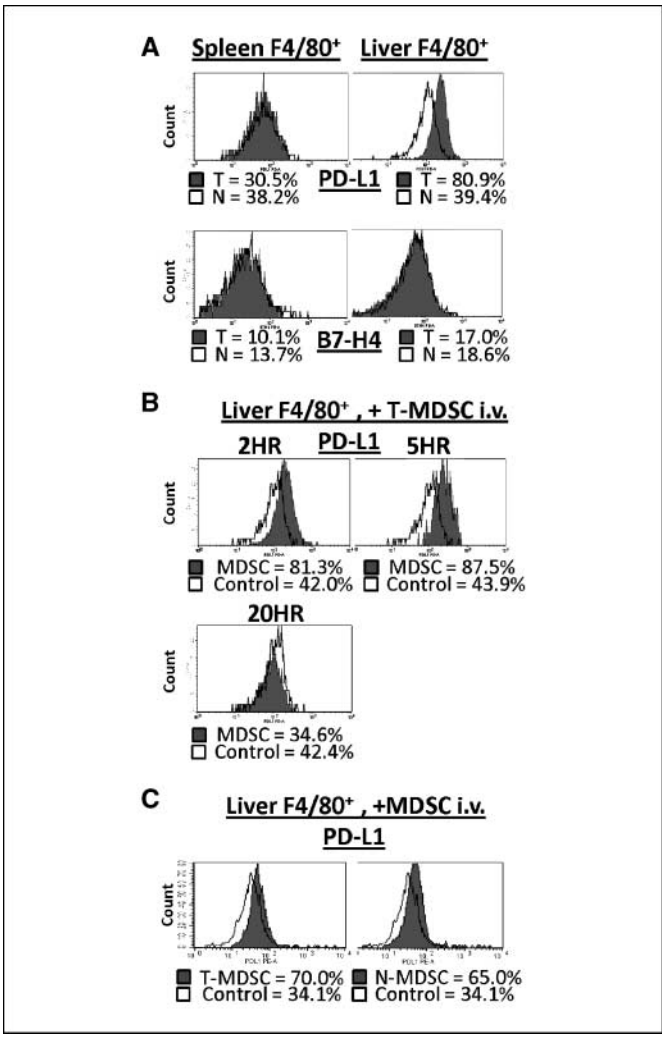


**Figure 5.** MDSC up-regulate PD-L1 surface expression on Kupffer cells. *A,* expression of PD-L1 or B7-H4 on DA-3 tumor–bearing (*T, gray*) or normal (*N, white*) mouse $F4/80^+$ cells from the liver or spleen. Gates were set so that isotype controls were no more than 5%. *B,* BALB/c mice were injected i.v. with saline (*Control, white*) or $15 \times 10^6$ DA-3 tumor–bearers' splenic MDSC (*MDSC, gray*), and 2, 5, or 20 h later, liver cells were harvested for analysis of PD-L1 expression on $F4/80^+$ cells. *C,* BALB/c mice were injected i.v. with saline (*Control, white*), $15 \times 10^6$ DA-3 tumor–bearers' splenic MDSC (*T-MDSC, gray*), or pooled $15 \times 10^6$ normal mouse splenic MDSC (*N-MDSC, gray*), and, 5 h later, liver cells were harvested for analysis of PD-L1 expression on $F4/80^+$ cells. Data are representative of at least three experiments.

Published OnlineFirst June 23, 2009; DOI: 10.1158/0008-5472.CAN-08-4625



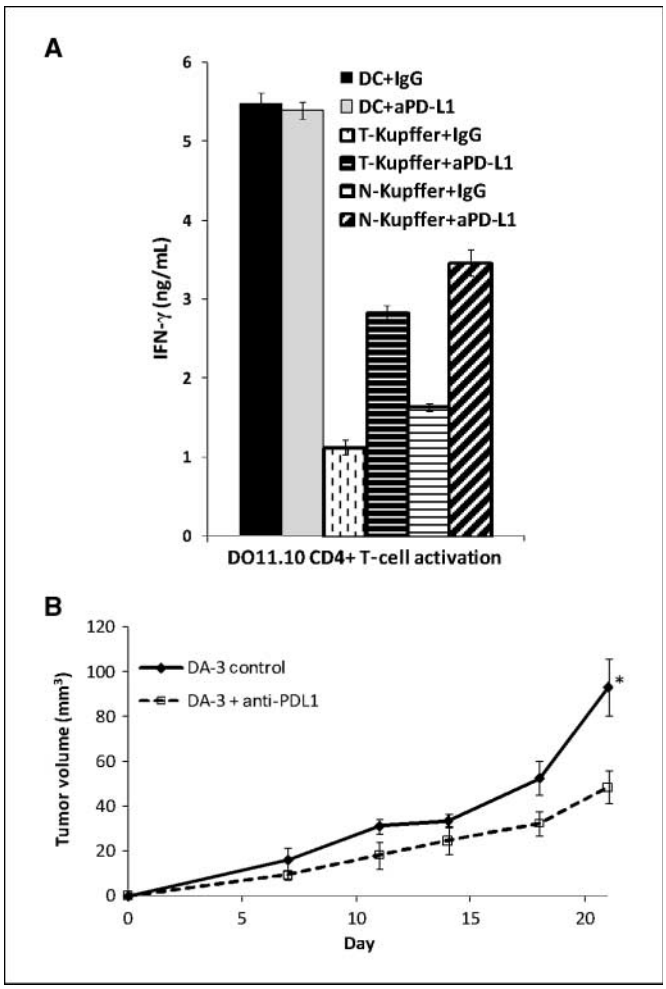


**Figure 6.** PD-L1 and immunosuppression. *A,* preactivated DO11.10 T cells were cultured with normal splenic dendritic cells (*DC*), tumor Kupffer cells (*T-Kupffer*), or normal Kupffer cells (*N-Kupffer*) in the presence of 5 μg/mL of ovalbumin, and F(ab′)$_2$ fragments of either isotype control (*IgG*) or a blocking antibody to PD-L1 (*aPD-L1*). IFN-γ was assayed in 4-d-old culture supernatants to assess the suppression of IFN-γ production by the PD-L1 pathway. Data is representative of at least three experiments. *B,* BALB/c mice were inoculated with DA-3 cells s.c. and then administered saline (*DA-3 control*) or 150 μg of anti–PD-L1 (*DA-3 + anti-PDL1)* twice a week beginning on day 3. *Bars,* SE (*, $P < 0.05$).

phenotype was affected in tumor-bearers. PD-L1 is a negative costimulatory molecule expressed in the liver by liver sinusoidal endothelial cells (42), Kupffer cells (42), and hepatocytes (43), and all have been shown to be capable of down-regulating T-cell responses and activation via this negative regulator. Furthermore, blocking this negative regulatory pathway has been shown to enhance immunity in certain pathologic states, such as viral clearance (42). Analyzing the levels of PD-L1 on Kupffer cells, we found a 2-fold higher expression on cells from tumor-bearing mice (Fig. 5). This up-regulation was specific to these liver macrophages, as splenic macrophages did not show a difference in PD-L1 expression. Furthermore, adoptive transfer of tumor-bearers' splenocytes or purified MDSC, from tumor-bearers' spleens or pooled normal spleens, into normal mice resulted in an up-regulation of PD-L1 on Kupffer cells. Thus, MDSC within the liver interact with Kupffer cells to up-regulate their expression of PD-L1. It is also important to note that although in some reports, PD-L1 expression was found on MDSC (44), in the tumor models we tested, MDSC were consistently negative for PD-L1, whereas Kupffer cells express relatively high levels. This may be due to a difference in tumor-derived factors between the tumor types, which may regulate the expression of PD-L1 on MDSC. The data presented also confirms previous reports that PD-L1 expression by Kupffer cells suppresses IFN-γ production by activated T-cells, and thus, potentially limits effective T-cell–dependent immune responses (Fig. 6).

This study reveals that systemic levels of MDSC are up-regulated in the livers of tumor-bearing mice, and that these cells can home to this organ in addition to other previously reported organ sites. The observed nests of MDSC in the livers of tumor-bearers, and the increased hematopoietic clonogenic activity, also suggest the possibility that they may develop in the liver in addition to just accumulating there. Furthermore, MDSC in the liver interact with Kupffer cells and augment their expression of PD-L1, a negative costimulatory molecule. MDSC in the liver likely also modulates other cells as this organ is known to harbor various immune-related cells, as was recently shown for MDSC interactions with natural killer cells from the liver (38). These findings open up new avenues to understanding how MDSC regulate immunity, as their effects on other cell populations can be organ-specific, and our understanding of their biology is applicable to various areas in which they have been described in addition to cancer, such as inflammation (7), transplantation (11), and infection (10).

## Disclosure of Potential Conflicts of Interest

No potential conflicts of interest were disclosed.

## Acknowledgments

Received 12/4/08; revised 4/17/09; accepted 5/4/09; published OnlineFirst 6/23/09.

**Grant support:** NIH grants R01CA25583 and F31GM079805, National Cancer Center predoctoral fellowship, and BD Biosciences Immunology Research grant.

The costs of publication of this article were defrayed in part by the payment of page charges. This article must therefore be hereby marked *advertisement* in accordance with 18 U.S.C. Section 1734 solely to indicate this fact.

We are particularly grateful to Drs. Carolyn Cray and Norman H. Altman from Comparative Pathology for their assistance and advice with tissue histology, Joy Prewitt from the Oncogenomics Core facility for help with the IVIS bioimager, and Jim Phillips from the Flow Cytometry Core facility. We also thank Taylor Schreiber for help with confocal imaging.

## References

1. Dunn GP, Old LJ, Schreiber RD. The three Es of cancer immunoediting. Annu Rev Immunol 2004;22:329–60.
2. Fu YX, Watson G, Jimenez JJ, Wang Y, Lopez DM. Expansion of immunoregulatory macrophages by granulocyte-macrophage colony-stimulating factor derived from a murine mammary tumor. Cancer Res 1990;50:227–34.
3. Watson GA, Fu YX, Lopez DM. Splenic macrophages from tumor-bearing mice co-expressing MAC-1 and MAC-2 antigens exert immunoregulatory functions via two distinct mechanisms. J Leukoc Biol 1991;49:126–38.
4. Gabrilovich DI, Nagaraj S. Myeloid-derived suppressor cells as regulators of the immune system. Nat Rev Immunol 2009;9:162–74.
5. Serafini P, Borrello I, Bronte V. Myeloid suppressor cells in cancer: recruitment, phenotype, properties, and mechanisms of immune suppression. Semin Cancer Biol 2006;16:53–65.
6. Ochoa AC, Zea AH, Hernandez C, Rodriguez PC. Arginase, prostaglandins, and myeloid-derived suppressor cells in renal cell carcinoma. Clin Cancer Res 2007;13:721–6s.
7. Haile LA, von Wasielewski R, Gamrekelashvili J, et al. Myeloid-derived suppressor cells in inflammatory bowel disease: a new immunoregulatory pathway. Gastroenterology 2008;135:871–81, 81 e1–5.

**8.** Makarenkova VP, Bansal V, Matta BM, Perez LA, Ochoa JB. CD11b+/Gr-1+ myeloid suppressor cells cause T cell dysfunction after traumatic stress. J Immunol 2006;176:2085–94.

**9.** Noel JG, Osterburg A, Wang Q, et al. Thermal injury elevates the inflammatory monocyte subpopulation in multiple compartments. Shock 2007;28:684–93.

**10.** Delano MJ, Scumpia PO, Weinstein JS, et al. MyD88-dependent expansion of an immature GR-1(+)CD11b(+) population induces T cell suppression and Th2 polarization in sepsis. J Exp Med 2007;204:1463–74.

**11.** Dugast AS, Haudebourg T, Coulon F, et al. Myeloid-derived suppressor cells accumulate in kidney allograft tolerance and specifically suppress effector T cell expansion. J Immunol 2008;180:7898–906.

**12.** Ilkovitch D, Lopez DM. Immune modulation by melanoma-derived factors. Exp Dermatol 2008;17:977–85.

**13.** Liu C, Yu S, Kappes J, et al. Expansion of spleen myeloid suppressor cells represses NK cell cytotoxicity in tumor-bearing host. Blood 2007;109:4336–42.

**14.** Sinha P, Clements VK, Bunt SK, Albelda SM, Ostrand-Rosenberg S. Cross-talk between myeloid-derived suppressor cells and macrophages subverts tumor immunity toward a type 2 response. J Immunol 2007;179:977–83.

**15.** Huang B, Pan PY, Li Q, et al. Gr-1+CD115+ immature myeloid suppressor cells mediate the development of tumor-induced T regulatory cells and T-cell anergy in tumor-bearing host. Cancer Res 2006;66:1123–31.

**16.** Saio M, Radoja S, Marino M, Frey AB. Tumor-infiltrating macrophages induce apoptosis in activated CD8(+) T cells by a mechanism requiring cell contact and mediated by both the cell-associated form of TNF and nitric oxide. J Immunol 2001;167:5583–93.

**17.** Kalchenko V, Shivtiel S, Malina V, et al. Use of lipophilic near-infrared dye in whole-body optical imaging of hematopoietic cell homing. J Biomed Opt 2006;11:050507-1–050507-3.

**18.** Fu YX, Watson GA, Kasahara M, Lopez DM. The role of tumor-derived cytokines on the immune system of mice bearing a mammary adenocarcinoma. I. Induction of regulatory macrophages in normal mice by the *in vivo* administration of rGM-CSF. J Immunol 1991;146:783–9.

**19.** Melani C, Chiodoni C, Forni G, Colombo MP. Myeloid cell expansion elicited by the progression of spontaneous mammary carcinomas in c-erbB-2 transgenic BALB/c mice suppresses immune reactivity. Blood 2003;102:2138–45.

**20.** Callery MP, Kamei T, Flye MW. Kupffer cell blockade inhibits induction of tolerance by the portal venous route. Transplantation 1989;47:1092–4.

**21.** Kryczek I, Zou L, Rodriguez P, et al. B7-4 expression identifies a novel suppressive macrophage population in human ovarian carcinoma. J Exp Med 2006;203:871–81.

**22.** Maier H, Isogawa M, Freeman GJ, Chisari FV. PD-1:PD-L1 interactions contribute to the functional suppression of virus-specific CD8+ T lymphocytes in the liver. J Immunol 2007;178:2714–20.

**23.** Keir ME, Butte MJ, Freeman GJ, Sharpe AH. PD-1 and its ligands in tolerance and immunity. Annu Rev Immunol 2008;26:677–704.

**24.** Li B, VanRoey M, Wang C, et al. Anti-programmed death-1 synergizes with granulocyte macrophage colony-stimulating factor-secreting tumor cell immunotherapy providing therapeutic benefit to mice with established tumors. Clin Cancer Res 2009;15:1623–34.

**25.** Wei S, Shreiner AB, Takeshita N, et al. Tumor-induced immune suppression of *in vivo* effector T-cell priming is mediated by the B7-1/PD-1 axis and transforming growth factor β. Cancer Res 2008;68:5432–8.

**26.** Youn JI, Nagaraj S, Collazo M, Gabrilovich DI. Subsets of myeloid-derived suppressor cells in tumor-bearing mice. J Immunol 2008;181:5791–802.

**27.** Filipazzi P, Valenti R, Huber V, et al. Identification of a new subset of myeloid suppressor cells in peripheral blood of melanoma patients with modulation by a granulocyte-macrophage colony-stimulation factor-based antitumor vaccine. J Clin Oncol 2007;25:2546–53.

**28.** Diaz-Montero CM, Salem ML, Nishimura MI, et al. Increased circulating myeloid-derived suppressor cells correlate with clinical cancer stage, metastatic tumor burden, and doxorubicin-cyclophosphamide chemotherapy. Cancer Immunol Immunother 2009;58:49–59.

**29.** Almand B, Clark JI, Nikitina E, et al. Increased production of immature myeloid cells in cancer patients: a mechanism of immunosuppression in cancer. J Immunol 2001;166:678–89.

**30.** Kusmartsev S, Su Z, Heiser A, et al. Reversal of myeloid cell-mediated immunosuppression in patients with metastatic renal cell carcinoma. Clin Cancer Res 2008;14:8270–8.

**31.** Hoechst B, Ormandy LA, Ballmaier M, et al. A new population of myeloid-derived suppressor cells in hepatocellular carcinoma patients induces CD4(+)CD25(+)Foxp3(+) T cells. Gastroenterology 2008;135:234–43.

**32.** Rodriguez PC, Hernandez CP, Quiceno D, et al. Arginase I in myeloid suppressor cells is induced by COX-2 in lung carcinoma. J Exp Med 2005;202:931–9.

**33.** Bronte V, Apolloni E, Cabrelle A, et al. Identification of a CD11b(+)/Gr-1(+)/CD31(+) myeloid progenitor capable of activating or suppressing CD8(+) T cells. Blood 2000;96:3838–46.

**34.** Ilkovitch D, Lopez DM. Urokinase-mediated recruitment of myeloid-derived suppressor cells and their suppressive mechanisms are blocked by MUC1/sec. Blood 2009;113:4729–39.

**35.** Pan PY, Wang GX, Yin B, et al. Reversion of immune tolerance in advanced malignancy: modulation of myeloid-derived suppressor cell development by blockade of stem-cell factor function. Blood 2008;111:219–28.

**36.** DuPre SA, Redelman D, Hunter KW, Jr. The mouse mammary carcinoma 4T1: characterization of the cellular landscape of primary tumours and metastatic tumour foci. Int J Exp Pathol 2007;88:351–60.

**37.** Tao K, Fang M, Alroy J, Sahagian GG. Imagable 4T1 model for the study of late stage breast cancer. BMC Cancer 2008;8:228.

**38.** Li H, Han Y, Guo Q, Zhang M, Cao X. Cancer-expanded myeloid-derived suppressor cells induce anergy of NK cells through membrane-bound TGF-β1. J Immunol 2009;182:240–9.

**39.** Dinapoli MR, Calderon CL, Lopez DM. The altered tumoricidal capacity of macrophages isolated from tumor-bearing mice is related to reduce expression of the inducible nitric oxide synthase gene. J Exp Med 1996;183:1323–9.

**40.** Watson GA, Lopez DM. Aberrant antigen presentation by macrophages from tumor-bearing mice is involved in the down-regulation of their T cell responses. J Immunol 1995;155:3124–34.

**41.** Sotomayor EM, Fu YX, Lopez-Cepero M, et al. Role of tumor-derived cytokines on the immune system of mice bearing a mammary adenocarcinoma. II. Down-regulation of macrophage-mediated cytotoxicity by tumor-derived granulocyte-macrophage colony-stimulating factor. J Immunol 1991;147:2816–23.

**42.** Iwai Y, Terawaki S, Ikegawa M, Okazaki T, Honjo T. PD-1 inhibits antiviral immunity at the effector phase in the liver. J Exp Med 2003;198:39–50.

**43.** Wahl C, Bochtler P, Chen L, Schirmbeck R, Reimann J. B7-1 on hepatocytes facilitates priming of specific CD8 T cells but limits the specific recall of primed responses. Gastroenterology 2008;135:980–8.

**44.** Liu Y, Zeng B, Zhang Z, Zhang Y, Yang R. B7-1 on myeloid-derived suppressor cells in immune suppression by a mouse model of ovarian cancer. Clin Immunol 2008;129:471–81.

Cancer Research
The Journal of Cancer Research (1916–1930) | The American Journal of Cancer (1931–1940)

AACR American Association for Cancer Research

# The Liver Is a Site for Tumor-Induced Myeloid-Derived Suppressor Cell Accumulation and Immunosuppression

Dan Ilkovitch and Diana M. Lopez

*Cancer Res* 2009;69:5514-5521. Published OnlineFirst June 23, 2009.